Mouse podoplanin supports adhesion and aggregation of platelets under arterial shear: a novel mechanism of haemostasis

Article

Accepted Version

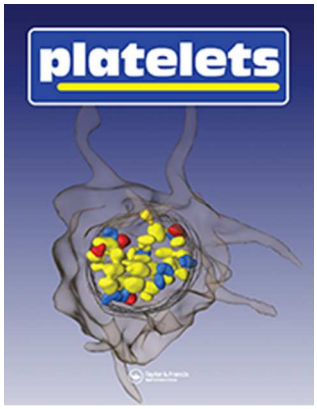

Mouse podoplanin supports adhesion and aggregation of platelets under arterial shear: a novel mechanism of haemostasis

Journal:	*Platelets*
Manuscript ID	CPLA-2017-0147.R1
Manuscript Type:	Original Article
Date Submitted by the Author:	n/a
Complete List of Authors:	Lombard, Stephanie; Birmingham University, Institute of Cardiovascular Sciences Pollitt, Alice ; University of Reading, Institute for Cardiovascular and Metabolic Research; Birmingham University, Institute of Cardiovascular Sciences Hughes, Craig; University of Reading, Institute for Cardiovascular and Metabolic Research; Birmingham University, Institute of Cardiovascular Sciences Di, Ying; Birmingham University, Institute of Cardiovascular Sciences Mckinnon, Thomas; Imperial College London, Department of Haematology O'Callaghan, Christopher; Wellcome Trust Centre for Human Genetics, Nuffield Department of Medicine Watson, Steve; Birmingham University, Institute of Cardiovascular Sciences
Keywords:	platelet activation, CLEC-2, podoplanin, platelet aggregation, capillary flow assay

Mouse podoplanin supports adhesion and aggregation of platelets under arterial shear: a novel mechanism of haemostasis

Stephanie E. Lombard[1], Alice Y. Pollitt[1,2], Craig E. Hughes[1,2], Ying Di[1], Tom Mckinnon[3], Chris A. O' Callaghan[4], Steve P. Watson[1]*.

[1] Centre for Cardiovascular Sciences, Institute for Biomedical Research, The College of Medical and Dental Sciences, University of Birmingham, Edgbaston, Birmingham B15 2TT, United Kingdom.

[2] Institute for Cardiovascular and Metabolic Research, School of Biological Sciences, Harborne Building, University of Reading, Whiteknights, Reading RG6 6AS, United Kingdom

[3] Faculty of Medicine, Department of Medicine, Commonwealth Building, Hammersmith Campus, Imperial, London

[4] Henry Wellcome Building for Molecular Physiology, University of Oxford, Roosevelt Drive, Oxford OX3 7BN, United Kingdom

* Corresponding authors: Steve P. Watson, Centre for Cardiovascular Sciences, Institute for Biomedical Research, College of Medical and Dental Sciences, University of Birmingham, Birmingham, UK. Phone: +44 (0) 121 414 6514. Email: S.P.Watson@bham.ac.uk

Alice Y Pollitt, Institute for Cardiovascular and Metabolic Research, School of Biological Sciences, Harborne Building, University of Reading, Whiteknights, Reading RG6 6AS, UK. Phone: 0118 378 8169; E-mail: a.pollitt@reading.ac.uk

Short title: Podoplanin supports platelet aggregation

Keywords: platelet activation, CLEC-2, podoplanin, platelet aggregation, capillary flow assay

Abstract

The Podoplanin-CLEC-2 axis is critical in mice for prevention of haemorrhage in the cerebral vasculature during mid-gestation. This raises the question as to how platelets are captured by podoplanin on neuroepithelial cells in a high shear environment. In this study, we demonstrate that mouse platelets form stable aggregates on mouse podoplanin at arterial shear through a CLEC-2 and Src kinase-dependent pathway. Adhesion and aggregation are also dependent on the platelet glycoprotein (GP) receptors, integrin αIIbβ3 and GPIb, and the feedback agonists ADP and thromboxane A_2 (TxA_2). CLEC-2 does not bind to von Willebrand factor (VWF) suggesting that the interaction with podoplanin is sufficient to both tether and activate platelets. Consistent with this, surface plasmon resonance measurements reveal that mouse CLEC-2 binds to mouse podoplanin with nanomolar affinity. The present findings demonstrate a novel pathway of haemostasis in which podoplanin supporting platelet capture and activation at arteriolar rates of shear.

Introduction

The C-type lectin-like receptor CLEC-2 is a type II transmembrane protein expressed on the surface of platelets, megakaryocytes and a subset of activated dendritic cells [1,2] The CLEC-2 cytosolic tail contains a single YxxL sequence known as a hemITAM which is phosphorylated following ligand engagement through recruitment of Src family and Syk tyrosine kinases [3-5]. This initiates a Syk kinase-driven signalling pathway which leads to powerful activation of platelets through PLCγ2 [6,7,5,8].

The interaction of platelet CLEC-2 with its endogenous ligand podoplanin plays a critical role in development of the cerebral vasculature and lymphatic system in mice [9-13]. Post-development, CLEC-2 and podoplanin are required for prevention of haemorrhage in high endothelial vessels and at sites of inflammatory challenge [14,15]. However, CLEC-2 is not thought to have a significant role in haemostasis, as tail bleeding times are not altered in mice deficient in the C-type lectin-like receptor [16,12,17]. This is consistent with the absence of a recognized ligand for CLEC-2 in the vasculature. The presence of podoplanin on a wide variety of cell types including lymphatic endothelial cells, type 1 alveolar cells, kidney podocytes and the choroid plexus epithelium, as well as its up-regulation on macrophages and T_H17 T-cells, suggests important roles for the podoplanin-CLEC-2 axis beyond the vasculature [18].

Mice deficient in CLEC-2 or podoplanin exhibit haemorrhaging in the brain during mid gestation [10]. Podoplanin is expressed at high level on the neuroepithelium in development but becomes restricted to the choroid plexus and brain lymphatic vessels during late gestation and in the adult brain. Haemorrhaging in the cerebrovasculature is also present in mice deficient in Syk and the αIIb-subunit of integrin αIIbβ3 suggesting that it is mediated through the loss of CLEC-2 driven platelet aggregation [10].

Intraventricular haemorrhaging (IVH) occurs in approximately 25% of human infants born with a birthweight of less than 1500 g [19] and is believed to be due to cardiovascular and respiratory instability. However, many of these infants also have severe thrombocytopenia, although there is no direct relationship between platelet count and IVH [20,21]. These results demonstrate the need to further understand the molecular basis of platelet activation in the cerebrovasculature during development.

Shear rates of flow in the cerebral arterioles in neonatal and adult mouse brains are in the order 1000 s^{-1} and above [22,23]. We have shown that recombinant human podoplanin captures and activates human platelets at venous but not arterial rates of shear [24], consistent with the relatively low affinity of human podoplanin and human CLEC-2 of 24.5 μM [25]. In contrast, in the present study we show that mouse podoplanin is able to support adhesion and aggregation of mouse platelets at arteriolar rates of shear due to a three orders of magnitude greater affinity of mouse podoplanin for mouse CLEC-2. This

suggests a fundamental difference in the role of podoplanin and CLEC-2 in mouse relative to human.

Methods

Materials

The following were from the sources shown: glass capillaries tubes (Cambridge UK), dasatinib (Sigma, Poole, UK), cangrelor (Medicines company, Place, UK), indomethacin (Sigma, Poole,UK), p0p/B antibody (Emfret, Germany); eptifibatide (Queen Elizabeth Hospital Pharmacy, UK); Polyclonal rabbit anti-VWF (Dako); anti-mouse CLEC-2 antibody (clone 17D9; Bio-Rad), and anti-mouse PDPN (clone 8.1.1; eBioscience). Other reagents were from previously described sources.

Mouse strains

Animal experimentation was performed with ethical approval from the UK Home Office, (PPL 70/8286). All experiments were performed on a C57Bl/6J background. Floxed CLEC-2 mice (CLEC-$2^{fl/fl}$) were crossed with PF4 Cre mice as previously described [9]. Controls were CLEC-$2^{fl/fl}$ mice.

Recombinant mouse podoplanin expression

Fc mPodoplanin (mPdpn-Fc) was generated as previously described [26]. The vector pHLsec was used for expression of His-tagged mPdpn (mPdpn-His). For expression and purification of the His-tagged fusion protein, the expression vector was transfected into 293T cells using polyethylenimine transfection. The fusion protein was purified from cell culture supernatants by affinity chromatography using Ni-NTA beads (Qiagen), eluted with 60% imidazole solution, and dialyzed into phosphate-buffered saline (PBS). Purity was determined by sodium dodecyl sulphate-polyacrylamide gel electrophoresis (SDS-PAGE) and western blotting using an anti-His tag antibody.

Recombinant mouse CLEC-2 expression

A fusion protein of amino acids 55-229 of the mCLEC-2 ECD fused to an N terminal 6xHIS tag was generated using the amplification primers GGAACCGGTCATCATCACCATCACCATCACCATACACAGCAAAAGTATCTA and CGTGGTACCTTAAAGCAGTTGGTCCACTCT. The PCR product was cloned into the expression vector pHLsec and expressed in 293T cells using polyethylenimine transfection. The fusion protein was purified from cell culture supernatants by affinity chromatography using a 1ml HisTrap HP (GE Healthcare) and eluted using imidazole solution and dialysed into PBS. Fusion protein purity was investigated by SDS-PAGE and western blotting with an anti-His antibody. The mCLEC-2-rFc plasmid was a kind gift from Sophie Acton and Shannon Turley [27]. This was used to make a stable cell line which secreted the recombinant protein into the cell media. mCLEC-2-rFc was purified in the same manner as mPdpn-Fc.

Expression of recombinant murine VWF

The cDNA for murine VWF (mVWF), previously cloned into the mammalian expression vector pcDNA3.1, was transiently transfected into HEK293T cells using 10mM polyethylenimine as previously described [28]. Four days post transfection, cell media was harvested and centrifuged at 4000*g* for 15 min to remove dead cells. Recombinant mVWF was partially purified by passing over an ion-exchange column packed with Fractogel-EMD-TMAE (Merck-Millipore) in 20mM Tris, 100mM NaCl, pH 7.8. Bound VWF was eluted with 500mM NaCl and following extensive dialysis into 20mM Tris, pH 7.8 at 4°C, was concentrated using 100kDa cut-off spin filters (Amicon, Peterborough, UK). The final VWF concentration was determined by VWF ELISA.

Blood isolation

Blood was drawn from the inferior vena cava of anaesthetized and then CO_2-asphyxiated mice into 5 U/mL heparin and 40 µM PPACK, and stained with 2 µM $DiOC_6$. Human blood was drawn into 4.5% sodium citrate (w/v). No difference was observed using the alternative anticoagulant combination 5 U/mL heparin and 40 µM PPACK.

Capillary flow assay

Glass capillaries with internal dimensions of 1 x 0.1 mm were coated with 100 µg/ml fibrillar Horm collagen or 100 µg/ml mPdpn-Fc overnight at 4°C and then blocked with 5mg/ml heat denatured bovine serum albumin (BSA) in PBS. Whole blood was incubated with the fluorescent dye $DiOC_6$ and inhibitors for 10 min at 37°C. Blood was perfused through a capillary at the desired shear rate for up to 4 min at 37°C as previously described [16].

Live imaging of platelet aggregate formation under flow was performed on an inverted stage microscope (DM IRB, Leica Microsystems Ltd, Milton Keynes UK) equipped with a digital camera (CoolSnap ES, Photometrics, Huntington Beach, CA) under fluorescent light for the duration of the experiment.

Dot Blot assay

A dot blot assay was used to test protein-ligand binding. The assay was carried out by dotting 0.1 µg of the target protein onto a nitrocellulose membrane (BioRad). After the dots were air dried, the membrane was blocked in 5% milk in PBS-Tween (0.5%: PBST) at room temperature for one hour. The membrane was incubated with ligand at 0.4 µg/ml in 2.5% milk in PBST overnight at 4°C. Next day, after washing, the membrane was incubated at room temperature with primary antibody of the ligand for 2 hours, followed by wash and then incubation with HRP conjugated secondary antibody for 1 hour. The membrane was visualized by ECL western blotting substrate (Thermo) on Li-COR Odyssey Fc system, with a developing time of 30 sec.

Surface plasmon resonance

Surface plasmon resonance (SPR) binding studies were conducted using a Biacore T200 machine (Biacore GE, Sweden) as described previously [3]. In brief, proteins were attached to the carboxymethylated dextran-coated surface of CM5 biosensor chips, using amine coupling chemistry. Experiments were performed in 10 mM HEPES pH 7.4, 150 mM NaCl, 3 mM EDTA and 0.005% polysorbate 20 surfactant. Non-specific interactions were controlled for by subtraction of the signal from a reference blank flow cell. To avoid avidity effects with podoplanin which was expressed as a dimeric Fc-fusion protein, experiments were only performed with podoplanin immobilized on the chip surface. Raw data was analysed using Scrubber2 (BioLogic Software Pty Ltd, Australia), and K_D values were obtained by nonlinear curve fitting using Graphpad Prism 5.

Analysis

Fluorescent images from the video capture of perfusion experiments were analysed using image J. Results from video capture are expressed as percentage area covered by platelets. Statistical analysis was performed using an unpaired Student's t-test or one-way ANOVA followed by Dunnett's post-test where appropriate, as indicated in the figure legends. Differences with $p < 0.05$ were considered statistically significant.

Results

Fc mPodoplanin (mPdpn-Fc) supports aggregation of mouse platelets at high shear

To investigate a possible role of podoplanin in platelet adhesion in the vasculature, we investigated the ability of a dimerized form of mouse podoplanin to support platelet aggregation in conditions of flow using an *in vitro* blood flow system. The high purity of the recombinant podoplanin (mPdpn-Fc), which is a recombinant Fc fusion of the mouse podoplanin extracellular domain, was investigated using SDS-PAGE under reducing and non-reducing conditions (Supplemental Figure 1).

Mouse blood was perfused over an immobilized monolayer of mPdpn-Fc using a range of venous and arterial shear rates (100 - 1000s^{-1}) (Figure 1A). A control recombinant Fc protein did not support platelet adhesion at any of the shear rates (not shown). Mouse platelets adhere and form small aggregates on a podoplanin-coated surface at 100s^{-1}. At the higher shear rate of 500s^{-1}, platelets form fewer but larger, distinct aggregates. At an arterial shear rate of 1000s^{-1}, podoplanin supported formation of large aggregates. There was no adhesion at 2000s^{-1} and above (not shown). Quantification of platelet coverage after 4 min of perfusion demonstrated a significant increase in percentage coverage at 1000s^{-1} compared with 100s^{-1} and 500s^{-1} (Figure 1B).

Fc mPodoplanin induced platelet adhesion is dependent on CLEC-2

To establish the role of CLEC-2 in adhesion and aggregation, blood from platelet-specific CLEC-2 deficient mice (PF4-Cre.CLEC-$2^{fl/fl}$) was perfused over mPdpn-Fc coated capillaries. Deletion of CLEC-2 abolished platelet adhesion at 100s^{-1} and 1000s^{-1} compared with CLEC-$2^{fl/fl}$ littermates (Figure 2A and B). In contrast, blood from PF4-Cre.CLEC-$2^{fl/fl}$ mice aggregated normally on a collagen-coated capillary relative to littermate controls in agreement with previous results (Figure 2A) [16].

Regulation of platelet aggregation on podoplanin

Pharmacological inhibitors were used to investigate the role of platelet receptors and their signalling pathways in platelet adhesion to immobilized podoplanin. The Src family kinase inhibitor dasatinib abolished aggregation on podoplanin leaving only single platelets (Figure 3A, B), consistent with a critical role for Src kinases in CLEC-2 signalling [26]. CLEC-2 signalling is also dependent on the feedback agonists TxA_2 and ADP [6,29]. In line with this, a combination of the cyclooxygenase inhibitor indomethacin and the $P2Y_{12}$ receptor antagonist, Cangrelor, blocked aggregation on mouse podoplanin at 1000s^{-1} leaving only single platelets and small platelet clumps (Figure 3A, B).

Aggregation of platelets is mediated by crosslinking of fibrinogen to integrin αIIbβ3 [30]. Inhibition of αIIbβ3 by the blocking peptide, epifibatide, markedly inhibited aggregation at 1000s^{-1} (Figure 3A). Blocking the GPIbα-subunit of the VWF receptor GPIb-IX-V by the

monoclonal antibody p0p/B also markedly reduced platelet aggregation, leaving small platelet clumps (Figure 3A, B). These results indicate that platelet aggregation on podoplanin is driven by CLEC-2-dependent activation of Src kinases leading to release of the feedback agonists ADP and TxA_2 and activation of integrin αIIbβ3. The GPIb-IX-V receptor mediates tethering and capture of platelets in the growing thrombus through interaction with VWF. The adhesion of single platelets in the presence of the GPIb blocking antibody indicates that this interaction is not required for initial platelet adhesion to podoplanin. Consistent with this, mouse VWF did not bind to mPdpn-Fc (Figure 3C). Binding of mouse VWF to collagen and mPdpn-Fc with mCLEC-2-Fc served as positive controls (Figure 3C).

Fc mPodoplanin (mPdpn-Fc) supports the aggregation of human platelets at venous rates of shear

The above results demonstrate the unexpected observation that mouse podoplanin can support adhesion and aggregation of mouse platelets at both venous and arterial rates of flow. The latter is in contrast to previous results for human podoplanin with human and mouse platelets [24,11]. To investigate whether mouse podoplanin is able to support adhesion and aggregation of human platelets, blood was perfused over a monolayer of mPdpn-Fc. Human platelets form small aggregates on mPdpn-Fc coated surface at $100s^{-1}$ but not at a shear rate of $300s^{-1}$ and above (not shown). Aggregation is reduced to single platelets in the presence of the Src kinase inhibitor, dasatinib (Figure 4A and B). The αIIbβ3 inhibitor, eptifibatide, blocked aggregation (Figure 4A and B).

Mouse CLEC-2 and mouse podoplanin interact with high affinity

We measured the binding affinity between mouse CLEC-2 and mouse podoplanin using SPR (Figure 5). In these studies we used dimeric mPdpn-Fc and monomeric podoplanin fused to a 6x Histidine tag (mPdpn-His). Both forms of mouse podoplanin showed a similar strong affinity to mCLEC-2-His of 15.3 $\pm$ 3.2 nM and 10.6 $\pm$ 1.3 nM respectively.

Discussion

This study demonstrates for the first time the ability of immobilized dimeric mouse podoplanin to initiate mouse platelet activation and aggregation at venous and arterial rates of shear through the C-type lectin-like receptor, CLEC-2. Aggregation on immobilized podoplanin is dependent on integrin αIIbβ3, the VWF receptor complex GPIb-IX-V, and the feedback mediators ADP and TxA_2 indicating that it involves classical haemostasis. The Src kinase inhibitor, dasatinib, blocks aggregate formation consistent with aggregation being driven by activation of the C-type lectin-like receptor.

Surface plasmon resonance demonstrates that mouse podoplanin binds to mouse CLEC-2 with nanomolar affinity providing a molecular basis for platelet capture at arterial flow rates. This contrasts with previous reports that human and mouse platelets are only able to form aggregates on human lymphatic endothelial cells, which express podoplanin, at venous rates of flow [11,24]. . The difference in interspecies interactions supports the reduced interaction of human platelets with recombinant mouse podoplanin observed in this study.

Several studies have described glycosylation of conserved threonine residues in the podoplanin platelet activation (PLAG) domains as important for the podoplanin mediated activation of platelets [31,32]. These extracellular PLAG domains of podoplanin are highly conserved between mouse and human podoplanin (The alignment of human and mouse podoplanin can be found in Supplemental Figure 2). Despite this conservation there are additional glycosylation sites throughout podoplanin which do not show conservation. One of note is the presence of a predicted N-glycosylation site which, while found in mouse podoplanin, is absent in human podoplanin [31].

It is recognized that the glycosylation of podoplanin is also dependent on the cell type in which is it expressed [33]. It is unclear to what extent differences in glycosylation impact on podoplanin function. A previous report demonstrated no difference between recombinant human podoplanin expressed by a human cell line compared to human podoplanin expressed by Chinese Hamster Ovary (CHO) cells to induce the aggregation of human platelets [34].

Classical haemostasis involves a number of stages. Platelets interact via GPIb with VWF immobilized to collagen and in turn collagen triggers platelet activation through the collagen receptor GPVI. VWF is critical for capture of platelets in the high shear environment in arteries and arterioles [35-37]. GPVI activates Src and Syk tyrosine kinases [38,39] leading to secretion of the feedback agonists ADP and TxA_2 [40,41]. A process of "inside out" signalling converts αIIbβ3 to an active confirmation and platelet-platelet interaction [42,43]. GPVI activates Src and Syk tyrosine kinases leading to activation of PLCγ2 and release of ADP and TxA_2 [29].

The present study provides evidence for a new pathway of haemostasis at high shear in which mouse podoplanin directly captures mouse platelets via CLEC-2. This supports stable adhesion and aggregation through a pathway that is dependent on granule secretion and TxA_2 formation. GPIb supports aggregation through tethering of platelets into the aggregate. We have previously demonstrated the importance of Src family kinases in CLEC-2 signalling, including in the adhesion of platelets to podoplanin through regulation of clustering of CLEC-2 and podoplanin [26].

Podoplanin is expressed on the neuroepithelium lining the cerebrovasculature in mice in mid-gestation [10] where it makes contact with platelets [22,23]. Loss of podoplanin expression on neuroepithelial cells phenocopies the haemorrhaging that seen in mice deficient in podoplanin or CLEC-2 [10]. Mice lacking the αIIb-subunit of the integrin αIIbβ3 also exhibit haemorrhaging in the cerebrovasculature although this is less severe than that that seen in mice deficient in CLEC-2 or podoplanin. This suggests a haemostatic and non-haemostatic role for the podoplanin-CLEC-2 axis in development of the cerebral vasculature.

Human platelets interact with podoplanin-expressing human lymphatic endothelial cells and with recombinant human podoplanin at low but not intermediate or high shear rates [24]. This is in line with the reported affinity between human podoplanin and human CLEC-2 of 24 μM [25], which is three orders of magnitude lower than that for mouse podoplanin and mouse CLEC-2. The difference in affinity leads to uncertainty as to whether the present findings can be extrapolated to the cerebrovasculature in human brain [44]. IVH is a common pathology in preterm neonatal babies who often exhibit low platelet counts [19-21]. The role of CLEC-2 in this process remains to be determined.

In conclusion, our study demonstrates the novel finding that mouse podoplanin initiates formation of stable platelet aggregates at high shear. We speculate that this is important during development of the mouse cerebrovasculature triggered by podoplanin on neuroepithelial cells and represents a specialised form of haemostasis.

Acknowledgements

The authors would like to thank Jamie R. McFarlane Webster for work done in the protein expression facility (PEF) in the University of Birmingham in the production of the recombinant forms of podoplanin, Prof. Bernard Nieswandt for kindly providing p0p/B antibody, Beata Grygielska for technical assistance, Maria Hoellerer for expression plasmids and Siân Lax for her assistance in preparing the manuscript.

Declaration of Interest

The authors declare no known conflicts of interest. SEL is a Wellcome Trust Prize Student (ref 099850). CEH and AYP were supported by the Wellcome Trust 088410. SPW holds a BHF Chair (CH/03/003).

References

[1] Suzuki-Inoue K CLEC-2, the novel platelet activation receptor and its internal ligand, podoplanin. Rinsho Ketsueki 2009;50:389-398.

[2] Lowe KL, Navarro-Nunez L, Benezech C, Nayar S, Kingston BL, Nieswandt B, Barone F, Watson SP, Buckley CD, Desanti GE The expression of mouse CLEC-2 on leucocyte subsets varies according to their anatomical location and inflammatory state. Eur J Immunol 2015;45:2484-2493.

[3] Hughes CE, Sinha U, Pandey A, Eble JA, O'Callaghan CA, Watson SP Critical Role for an acidic amino acid region in platelet signaling by the HemITAM (hemi-immunoreceptor tyrosine-based activation motif) containing receptor CLEC-2 (C-type lectin receptor-2). The Journal of biological chemistry 2013;288:5127-5135.

[4] Spalton JC, Mori J, Pollitt AY, Hughes CE, Eble JA, Watson SP The novel Syk inhibitor R406 reveals mechanistic differences in the initiation of GPVI and CLEC-2 signaling in platelets. Journal of thrombosis and haemostasis : JTH 2009;7:1192-1199.

[5] Severin S, Pollitt AY, Navarro-Nunez L, Nash CA, Mourao-Sa D, Eble JA, Senis YA, Watson SP Syk-dependent phosphorylation of CLEC-2: a novel mechanism of hem-immunoreceptor tyrosine-based activation motif signaling. The Journal of biological chemistry 2011;286:4107-4116.

[6] Pollitt AY, Grygielska B, Leblond B, Desire L, Eble JA, Watson SP Phosphorylation of CLEC-2 is dependent on lipid rafts, actin polymerization, secondary mediators, and Rac. Blood 2010;115:2938-2946.

[7] Suzuki-Inoue K, Fuller GL, Garcia A, Eble JA, Pohlmann S, Inoue O, Gartner TK, Hughan SC, Pearce AC, Laing GD, Theakston RD, Schweighoffer E, Zitzmann N, Morita T, Tybulewicz VL, Ozaki Y, Watson SP A novel Syk-dependent mechanism of platelet activation by the C-type lectin receptor CLEC-2. Blood 2006;107:542-549.

[8] Suzuki-Inoue K, Kato Y, Inoue O, Kaneko MK, Mishima K, Yatomi Y, Yamazaki Y, Narimatsu H, Ozaki Y Involvement of the snake toxin receptor CLEC-2, in podoplanin-mediated platelet activation, by cancer cells. The Journal of biological chemistry 2007;282:25993-26001.

[9] Finney BA, Schweighoffer E, Navarro-Nunez L, Benezech C, Barone F, Hughes CE, Langan SA, Lowe KL, Pollitt AY, Mourao-Sa D, Sheardown S, Nash GB, Smithers N, Reis e Sousa C, Tybulewicz VL, Watson SP CLEC-2 and Syk in the megakaryocytic/platelet lineage are essential for development. Blood 2012;119:1747-1756.

[10] Lowe KL, Finney BA, Deppermann C, Hagerling R, Gazit SL, Frampton J, Buckley C, Camerer E, Nieswandt B, Kiefer F, Watson SP Podoplanin and CLEC-2 drive cerebrovascular patterning and integrity during development. Blood 2015;125:3769-3777.

[11] Bertozzi CC, Schmaier AA, Mericko P, Hess PR, Zou Z, Chen M, Chen CY, Xu B, Lu MM, Zhou D, Sebzda E, Santore MT, Merianos DJ, Stadtfeld M, Flake AW, Graf T, Skoda R, Maltzman JS, Koretzky GA, Kahn ML Platelets regulate lymphatic vascular development through CLEC-2-SLP-76 signaling. Blood 2010;116:661-670.

[12] Suzuki-Inoue K, Inoue O, Ding G, Nishimura S, Hokamura K, Eto K, Kashiwagi H, Tomiyama Y, Yatomi Y, Umemura K, Shin Y, Hirashima M, Ozaki Y Essential in vivo roles of the C-type lectin receptor CLEC-2: embryonic/neonatal lethality of CLEC-2-deficient mice by blood/lymphatic misconnections and impaired thrombus formation of CLEC-2-deficient platelets. The Journal of biological chemistry 2010;285:24494-24507.

[13] Ichise H, Ichise T, Ohtani O, Yoshida N Phospholipase Cgamma2 is necessary for separation of blood and lymphatic vasculature in mice. Development 2009;136:191-195.

[14] Herzog BH, Fu J, Wilson SJ, Hess PR, Sen A, McDaniel JM, Pan Y, Sheng M, Yago T, Silasi-Mansat R, McGee S, May F, Nieswandt B, Morris AJ, Lupu F, Coughlin SR, McEver RP, Chen H, Kahn ML, Xia L Podoplanin maintains high endothelial venule integrity by interacting with platelet CLEC-2. Nature 2013;502:105-109.

[15] Hitchcock JR, Cook CN, Bobat S, Ross EA, Flores-Langarica A, Lowe KL, Khan M, Dominguez-Medina CC, Lax S, Carvalho-Gaspar M, Hubscher S, Rainger GE, Cobbold M, Buckley CD, Mitchell TJ, Mitchell A, Jones ND, Van Rooijen N, Kirchhofer D, Henderson IR, Adams DH, Watson SP,

Cunningham AF Inflammation drives thrombosis after Salmonella infection via CLEC-2 on platelets. J Clin Invest 2015;125:4429-4446.
[16] Hughes CE, Navarro-Nunez L, Finney BA, Mourao-Sa D, Pollitt AY, Watson SP CLEC-2 is not required for platelet aggregation at arteriolar shear. Journal of thrombosis and haemostasis : JTH 2010;8:2328-2332.
[17] Bender M, May F, Lorenz V, Thielmann I, Hagedorn I, Finney BA, Vogtle T, Remer K, Braun A, Bosl M, Watson SP, Nieswandt B Combined in vivo depletion of glycoprotein VI and C-type lectin-like receptor 2 severely compromises hemostasis and abrogates arterial thrombosis in mice. Arterioscler Thromb Vasc Biol 2013;33:926-934.
[18] Hou TZ, Bystrom J, Sherlock JP, Qureshi O, Parnell SM, Anderson G, Gilroy DW, Buckley CD A distinct subset of podoplanin (gp38) expressing F4/80+ macrophages mediate phagocytosis and are induced following zymosan peritonitis. FEBS letters 2010;584:3955-3961.
[19] Horbar JD, Badger GJ, Carpenter JH, Fanaroff AA, Kilpatrick S, LaCorte M, Phibbs R, Soll RF, Members of the Vermont Oxford N Trends in mortality and morbidity for very low birth weight infants, 1991-1999. Pediatrics 2002;110:143-151.
[20] Stanworth SJ Thrombocytopenia, bleeding, and use of platelet transfusions in sick neonates. Hematology Am Soc Hematol Educ Program 2012;2012:512-516.
[21] Ferrer-Marin F, Stanworth S, Josephson C, Sola-Visner M Distinct differences in platelet production and function between neonates and adults: implications for platelet transfusion practice. Transfusion 2013;53:2814-2821; quiz 2813.
[22] Wang DB, Blocher NC, Spence ME, Rovainen CM, Woolsey TA Development and remodeling of cerebral blood vessels and their flow in postnatal mice observed with in vivo videomicroscopy. J Cereb Blood Flow Metab 1992;12:935-946.
[23] Rovainen CM, Wang DB, Woolsey TA Strobe epi-illumination of fluorescent beads indicates similar velocities and wall shear rates in brain arterioles of newborn and adult mice. Microvasc Res 1992;43:235-239.
[24] Navarro-Nunez L, Pollitt AY, Lowe K, Latif A, Nash GB, Watson SP Platelet adhesion to podoplanin under flow is mediated by the receptor CLEC-2 and stabilised by Src/Syk-dependent platelet signalling. Thromb Haemost 2015;113:1109-1120.
[25] Christou CM, Pearce AC, Watson AA, Mistry AR, Pollitt AY, Fenton-May AE, Johnson LA, Jackson DG, Watson SP, O'Callaghan CA Renal cells activate the platelet receptor CLEC-2 through podoplanin. The Biochemical journal 2008;411:133-140.
[26] Pollitt AY, Poulter NS, Gitz E, Navarro-Nunez L, Wang YJ, Hughes CE, Thomas SG, Nieswandt B, Douglas MR, Owen DM, Jackson DG, Dustin ML, Watson SP Syk and Src family kinases regulate C-type lectin receptor 2 (CLEC-2)-mediated clustering of podoplanin and platelet adhesion to lymphatic endothelial cells. The Journal of biological chemistry 2014;289:35695-35710.
[27] Acton Sophie E, Astarita Jillian L, Malhotra D, Lukacs-Kornek V, Franz B, Hess Paul R, Jakus Z, Kuligowski M, Fletcher Anne L, Elpek Kutlu G, Bellemare-Pelletier A, Sceats L, Reynoso Erika D, Gonzalez Santiago F, Graham Daniel B, Chang J, Peters A, Woodruff M, Kim Y-A, Swat W, Morita T, Kuchroo V, Carroll Michael C, Kahn Mark L, Wucherpfennig Kai W, Turley Shannon J Podoplanin-Rich Stromal Networks Induce Dendritic Cell Motility via Activation of the C-type Lectin Receptor CLEC-2. Immunity 2012;37:276-289.
[28] Nowak AA, Canis K, Riddell A, Laffan MA, McKinnon TA O-linked glycosylation of von Willebrand factor modulates the interaction with platelet receptor glycoprotein Ib under static and shear stress conditions. Blood 2012;120:214-222.
[29] Borgognone A, Navarro-Nunez L, Correia JN, Pollitt AY, Thomas SG, Eble JA, Pulcinelli FM, Madhani M, Watson SP CLEC-2-dependent activation of mouse platelets is weakly inhibited by cAMP but not by cGMP. Journal of thrombosis and haemostasis : JTH 2014;12:550-559.
[30] Li Z, Delaney MK, O'Brien KA, Du X Signaling during platelet adhesion and activation. Arterioscler Thromb Vasc Biol 2010;30:2341-2349.

[31] Kaneko MK, Kato Y, Kitano T, Osawa M Conservation of a platelet activating domain of Aggrus/podoplanin as a platelet aggregation-inducing factor. Gene 2006;378:52-57.
[32] Kato Y, Fujita N, Kunita A, Sato S, Kaneko M, Osawa M, Tsuruo T Molecular identification of Aggrus/T1alpha as a platelet aggregation-inducing factor expressed in colorectal tumors. The Journal of biological chemistry 2003;278:51599-51605.
[33] Martin-Villar E, Fernandez-Munoz B, Parsons M, Yurrita MM, Megias D, Perez-Gomez E, Jones GE, Quintanilla M Podoplanin associates with CD44 to promote directional cell migration. Mol Biol Cell 2010;21:4387-4399.
[34] Kaneko MK, Kato Y, Kameyama A, Ito H, Kuno A, Hirabayashi J, Kubota T, Amano K, Chiba Y, Hasegawa Y, Sasagawa I, Mishima K, Narimatsu H Functional glycosylation of human podoplanin: glycan structure of platelet aggregation-inducing factor. FEBS letters 2007;581:331-336.
[35] Savage B, Saldivar E, Ruggeri ZM Initiation of platelet adhesion by arrest onto fibrinogen or translocation on von Willebrand factor. Cell 1996;84:289-297.
[36] Lopez JA, Dong JF Structure and function of the glycoprotein Ib-IX-V complex. Curr Opin Hematol 1997;4:323-329.
[37] Du X Signaling and regulation of the platelet glycoprotein Ib-IX-V complex. Curr Opin Hematol 2007;14:262-269.
[38] Senis YA, Mazharian A, Mori J Src family kinases: at the forefront of platelet activation. Blood 2014;124:2013-2024.
[39] Manne BK, Badolia R, Dangelmaier C, Eble JA, Ellmeier W, Kahn M, Kunapuli SP Distinct pathways regulate Syk protein activation downstream of immune tyrosine activation motif (ITAM) and hemITAM receptors in platelets. The Journal of biological chemistry 2015;290:11557-11568.
[40] Ren Q, Ye S, Whiteheart SW The platelet release reaction: just when you thought platelet secretion was simple. Curr Opin Hematol 2008;15:537-541.
[41] Reed GL, Fitzgerald ML, Polgar J Molecular mechanisms of platelet exocytosis: insights into the "secrete" life of thrombocytes. Blood 2000;96:3334-3342.
[42] Coller BS, Shattil SJ The GPIIb/IIIa (integrin alphaIIbbeta3) odyssey: a technology-driven saga of a receptor with twists, turns, and even a bend. Blood 2008;112:3011-3025.
[43] Shattil SJ, Kim C, Ginsberg MH The final steps of integrin activation: the end game. Nat Rev Mol Cell Biol 2010;11:288-300.
[44] Seymour RS, Bosiocic V, Snelling EP Fossil skulls reveal that blood flow rate to the brain increased faster than brain volume during human evolution. Royal Society Open Science 2016;3:160305.

Figures

Figure 1: Fc mPodoplanin (mPdpn-Fc) supports the aggregation of mouse platelets at high shear

A. Anticoagulated blood from wild-type mice was perfused through mPdpn-Fc-coated capillary tubes at the indicated shear rates. Platelets were fluorescently labelled with $DiOC_6$ before being perfused. Representative images were taken in real time by fluorescence microscopy. Arrow indicates the direction of flow. Scale bar 20 µm. Images are representative of 4 independent experiments. B. (i) Quantitation of mouse platelet area coverage following blood perfusion. Statistical analysis preformed using a one way ANOVA followed by a Dunnett's multiple comparisons test (*=p<0.05, **=p<0.01). The threshold image at 4 minutes is presented in the right hand panel. Error bars represent standard deviation.

Figure 2: Fc mpodoplanin (mPdpn-Fc) mediated platelet aggregation is dependent on the platelet receptor CLEC-2

A. Anticoagulated blood from PF4-Cre.CLEC-$2^{fl/fl}$ mice and CLEC-$2^{fl/fl}$ littermates was perfused through mPdpn-Fc and collagen-coated capillary tubes at the indicated shear rates. Platelets were fluorescently labelled with $DiOC_6$ before being perfused. Representative images were taken in real time by fluorescence microscopy. Arrow indicates the direction of flow. Scale bar 20 µm. Images are representative of 3 independent experiments. B. Quantitation of platelet coverage following blood perfusion. Statistical analysis was performed using an unpaired one tailed t test (*** = p<0.001). Error bars represent the standard deviation.

Figure 3: Effect of inhibitors on platelet aggregation on podoplanin under shear

A. Anticoagulated wild type (WT) mouse blood was perfused through mPdpn-Fc -coated capillary tubes at $1000s^{-1}$. Platelets were fluorescently labelled with $DiOC_6$ before being perfused and ten images taken post perfusion, with representative images shown: vehicle control image (Veh: DMSO), Dasatinib (Das: 10 µM), eptifibatide (Eptifib: 9 µM), Indomethacin (Indo: 10 µM) and Cangrelor (Cang: 1 µM), p0p/B antibody (50 µg/ml). Arrow indicates the direction of flow. Scale bar 20 µm. Images are representative of 4 independent experiments. B. Quantitation of platelet coverage following blood perfusion. Statistical analysis was performed using a one way ANOVA followed by a Dunnett's multiple comparisons test to the vehicle control, error bars represent standard deviation. * = p<0.05, ** = p<0.01, *** = p<0.001. C. Dot blot assay to determine ligand binding. 0.1 µg of protein (collagen, mPdpn-Fc and mCLEC-2-Fc) was air dried to nitrocellulose membrane. Following incubation with ligand (VWF, mCLEC-2-Fc and mPdpn-Fc) bound ligand was determined using the indicated antibodies.

Figure 4: Fc mPodoplanin supports aggregation of human platelets at low shear

A. Anticoagulated blood from human was perfused through Fc mpodoplanin (mPdpn-Fc)-coated capillary tubes at the indicated shear rates. Platelets were fluorescently labelled with $DiOC_6$ before being perfused. Representative images were taken in real time by fluorescence microscopy at $100s^{-1}$: vehicle control (Veh: DMSO), dasatinib (Das: 10 µM), eptifibatide (Eptifib: 9 µM). Arrow indicates the direction of flow. Scale bar 20 µm. Error bars represent standard deviation. Images are representative of 3 independent experiments. B. Quantitation of human platelet coverage following blood perfusion. Statistical analysis was performed using a one way ANOVA followed by a Dunnett's multiple comparisons test (* = $p<0.05$, ** = $p<0.01$). Error bars represent standard deviation.

Figure 5: Mouse CLEC-2 and mouse podoplanin interact directly with high affinity

A. Sensorgram from equilibrium–based binding experiment after subtraction of the signal from a control flow cell surface. Different concentrations of CLEC-2 were injected over surfaces coupled with Fc mouse podoplanin (mPdpn-Fc) and His tagged mouse podoplanin (mPdpn-His). The dissociation phase of the sensorgrams is observed following a 10 minute injection period, indicated by the closed arrow heads. Start of the flow cell surface regeneration is indicated on the sensograms by the open arrow heads. B. Plot of the equilibrium binding response from the sensorgram of mPdpn-Fc and mPdpn-His as a function of CLEC-2 concentration. The curve is the best fit to the experimental data as calculated by GraphPad Prism 5. The affinity between mouse CLEC-2 and mouse podoplanin was calculated to be 15.3 ± 3.2 nM when using mPdpn-Fc and 10.6 ± 1.3 nM when using mPdpn-His. C. Equilibrium binding response of mPdpn-Fc and mPdpn-His as a function of CLEC-2 concentration presented as a log-scale.

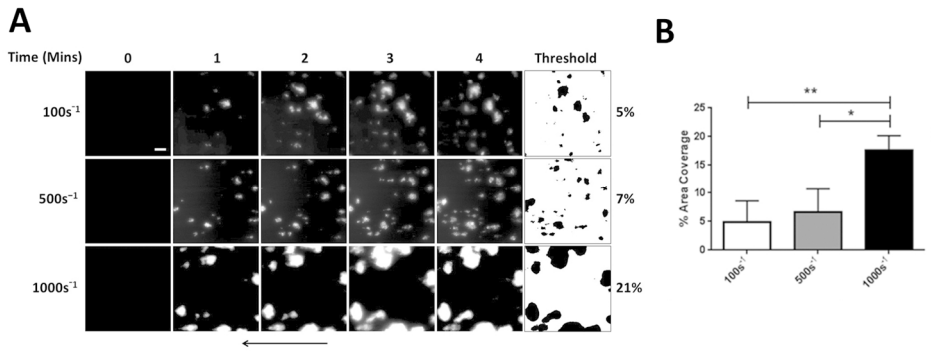

Figure 1: Fc mPodoplanin (mPdpn-Fc) supports the aggregation of mouse platelets at high shear
A. Anticoagulated blood from wild-type mice was perfused through mPdpn-Fc-coated capillary tubes at the indicated shear rates. Platelets were fluorescently labelled with DiOC6 before being perfused. Representative images were taken in real time by fluorescence microscopy. Arrow indicates the direction of flow. Scale bar 20 μm. Images are representative of 4 independent experiments. B. (i) Quantitation of mouse platelet area coverage following blood perfusion. Statistical analysis preformed using a one way ANOVA followed by a Dunnett's multiple comparisons test (*=p<0.05, **=p<0.01). The threshold image at 4 minutes is presented in the right hand panel. Error bars represent standard deviation.

150x112mm (300 x 300 DPI)

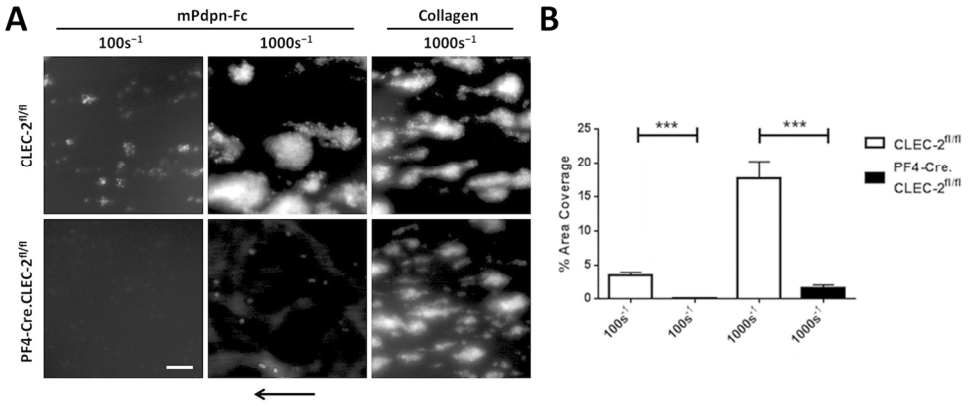

Figure 2: Fc mpodoplanin (mPdpn-Fc) mediated platelet aggregation is dependent on the platelet receptor CLEC-2

A. Anticoagulated blood from PF4-Cre.CLEC-2fl/fl mice and CLEC-2fl/fl littermates was perfused through mPdpn-Fc and collagen-coated capillary tubes at the indicated shear rates. Platelets were fluorescently labelled with DiOC6 before being perfused. Representative images were taken in real time by fluorescence microscopy. Arrow indicates the direction of flow. Scale bar 20 μm. Images are representative of 3 independent experiments. B. Quantitation of platelet coverage following blood perfusion. Statistical analysis was performed using an unpaired one tailed t test (*** = $p<0.001$). Error bars represent the standard deviation.

150x112mm (300 x 300 DPI)

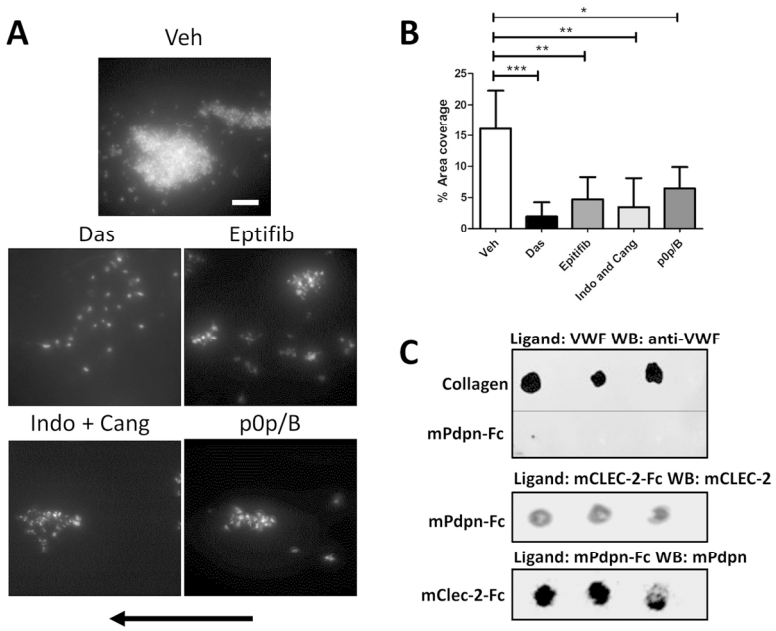

Figure 3: Effect of inhibitors on platelet aggregation on podoplanin under shear
A. Anticoagulated wild type (WT) mouse blood was perfused through mPdpn-Fc -coated capillary tubes at 1000s-1. Platelets were fluorescently labelled with DiOC6 before being perfused and ten images taken post perfusion, with representative images shown: vehicle control image (Veh: DMSO), Dasatinib (Das: 10 μM), eptifibatide (Eptifib: 9 μM), Indomethacin (Indo: 10 μM) and Cangrelor (Cang: 1 μM), p0p/B antibody (50 μg/ml). Arrow indicates the direction of flow. Scale bar 20 μm. Images are representative of 4 independent experiments. B. Quantitation of platelet coverage following blood perfusion. Statistical analysis was performed using a one way ANOVA followed by a Dunnett's multiple comparisons test to the vehicle control, error bars represent standard deviation. * = $p<0.05$, ** = $p<0.01$, *** = $p<0.001$. C. Dot blot assay to determine ligand binding. 0.1 μg of protein (collagen, mPdpn-Fc and mCLEC-2-Fc) was air dried to nitrocellulose membrane. Following incubation with ligand (VWF, mCLEC-2-Fc and mPdpn-Fc) bound ligand was determined using the indicated antibodies.

150x112mm (300 x 300 DPI)

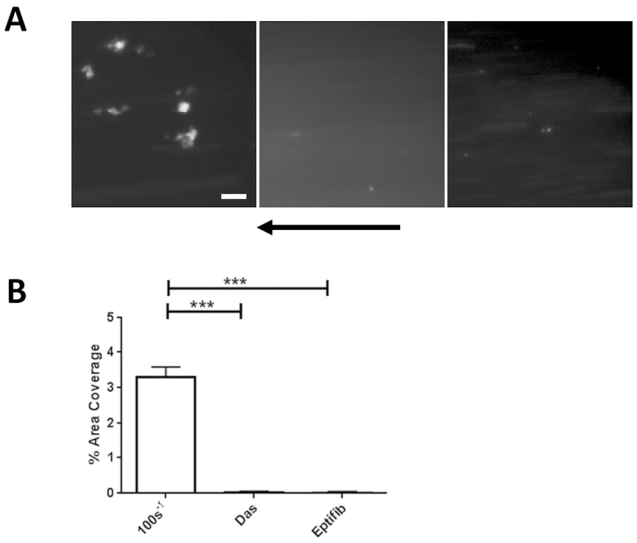

Figure 4: Fc mPodoplanin supports aggregation of human platelets at low shear
A. Anticoagulated blood from human was perfused through Fc mpodoplanin (mPdpn-Fc)-coated capillary tubes at the indicated shear rates. Platelets were fluorescently labelled with DiOC6 before being perfused. Representative images were taken in real time by fluorescence microscopy at 100s-1: vehicle control (Veh: DMSO), dasatinib (Das: 10 μM), eptifibatide (Eptifib: 9 μM). Arrow indicates the direction of flow. Scale bar 20 μm. Error bars represent standard deviation. Images are representative of 3 independent experiments. B. Quantitation of human platelet coverage following blood perfusion. Statistical analysis was performed using a one way ANOVA followed by a Dunnett's multiple comparisons test (* = $p<0.05$, ** = $p<0.01$). Error bars represent standard deviation.

150x112mm (300 x 300 DPI)

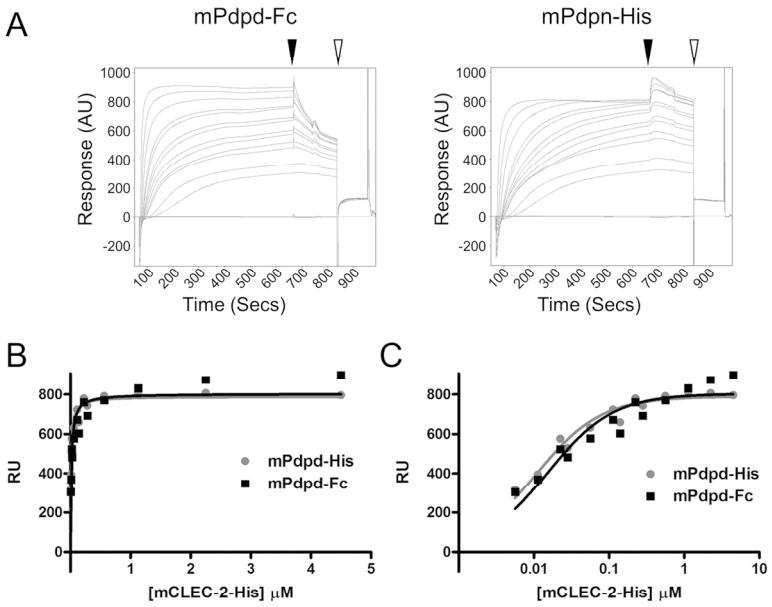

Figure 5: Mouse CLEC-2 and mouse podoplanin interact directly with high affinity
A. Sensorgram from equilibrium–based binding experiment after subtraction of the signal from a control flow cell surface. Different concentrations of CLEC-2 were injected over surfaces coupled with Fc mouse podoplanin (mPdpn-Fc) and His tagged mouse podoplanin (mPdpn-His). The dissociation phase of the sensorgrams is observed following a 10 minute injection period, indicated by the closed arrow heads. Start of the flow cell surface regeneration is indicated on the sensograms by the open arrow heads. B. Plot of the equilibrium binding response from the sensorgram of mPdpn-Fc and mPdpn-His as a function of CLEC-2 concentration. The curve is the best fit to the experimental data as calculated by GraphPad Prism 5. The affinity between mouse CLEC-2 and mouse podoplanin was calculated to be 15.3 ± 3.2 nM when using mPdpn-Fc and 10.6 ± 1.3 nM when using mPdpn-His. C. Equilibrium binding response of mPdpn-Fc and mPdpn-His as a function of CLEC-2 concentration presented as a log-scale.

150x112mm (300 x 300 DPI)

Supplemental Figure 1: Elution fractions of recombinant FcmPdpn.

The purity of the recombinant mouse podoplanin extracellular domain expressed as an Fc fusion was determined under reducing and non-reducing SDS-PAGE followed by Coomassie protein staining. Under non-reducing condition the Fc fusion migrates at a high molecular weight dimer. Under reducing conditions reduction of the Fc intra-chain disulphide bonds in the recombinant protein occurs leading to a lower molecular weight monomer.

Supplemental Figure 2: Protein alignment of mouse and human podoplanin.

Podoplanin sequences from human and mouse were aligned using TCoffee web-based software [1] and presented using ESPript3 [2]. The extracellular domain contains conserved threonine residues within the platelet activating (PLAG) domains 1 and 3, indicated by a *. The predicted N-glycosylation site in mouse podoplanin is indicated by a box. The signal peptide and transmembrane domain are indicated.

Supplementary references

[1] Di Tommaso P, Moretti S, Xenarios I, Orobitg M, Montanyola A, Chang JM, Taly JF, Notredame C T-Coffee: a web server for the multiple sequence alignment of protein and RNA sequences using structural information and homology extension. Nucleic acids research 2011;39:W13-17.
[2] Robert X, Gouet P Deciphering key features in protein structures with the new ENDscript server. Nucleic acids research 2014;42:W320-324.

Figure S1

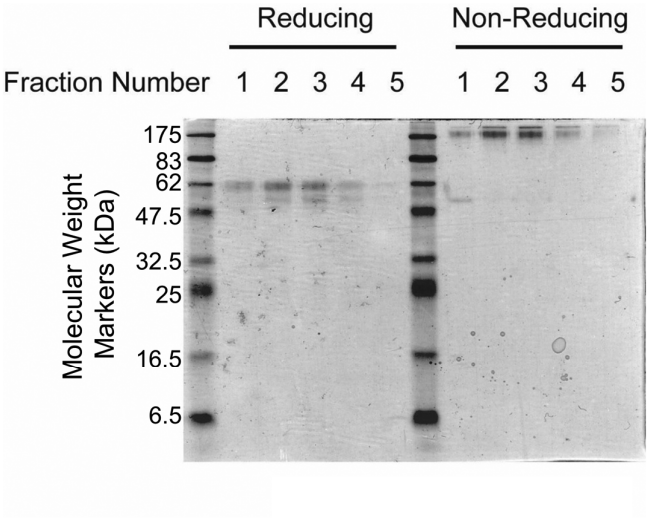

Figure S2